Orissa Journal of Physics
ISSN 0974-8202

Vol. 33, No.1
February 2026
pp. 118-130

Nonlinear stability and bifurcation analysis in prime number distributions

CHARLI CHINMAYEE PAL† AND PRASANTA KUMAR MAHAPATRA

Department of Physics, Siksha 'O' Anusandhan, deemed to be University, Bhubaneswar-751030, India

Abstract: We propose a nonlinear dynamical framework for analyzing the distribution of prime numbers along the number line. Rigorous lower and upper bounds for the prime counting function are used to construct corresponding bounds on the prime density, yielding substantially improved accuracy over existing approximations and consistently enclosing the exact values. A single-particle wave function is formulated from the bounded prime density, and the associated interaction potential is derived using the Schrödinger equation. The resulting potentials are singular and intrinsically nonlinear, exhibiting distinct attractive and repulsive regimes. An equivalent classical Hamiltonian system governed by these potentials is then examined to study phase-space trajectories, equilibrium points, and their stability properties. The analysis reveals the occurrence of fold and blue-sky bifurcations, indicating the presence of an underlying nonlinear dynamical structure governing prime number distribution.
PACS: 02.30.Oz, 05.45.-a, 45.20.Jj, 47.10.Df, 65.40.De

Keywords: Prime counting function, Prime density, Fixed point analysis, Bifurcation phenomena
E-mail: charlichinmayee24@gmail.com

1. INTRODUCTION:

Prime numbers have fascinated the scientific community since the earliest stages of human civilization, owing to their seemingly irregular and complex distribution along the number line. Despite their deterministic definition, primes exhibit a striking interplay between randomness and regularity, a feature that has remained enigmatic even after centuries of rigorous investigation. This dual nature has motivated researchers to look beyond traditional analytic approaches and explore alternative frameworks capable of capturing the intricate structure of prime distributions. While the Prime Number Theorem accurately describes the average density of primes through a linear logarithmic relation, it fails to account for the pronounced fluctuations and irregular spacing observed locally. These deviations from the mean behaviour exhibit features reminiscent of nonlinear and chaotic dynamical systems, such as intermittency, clustering, and scale-dependent variability. Consequently, several studies [1-11] have investigated prime

sequences using tools from nonlinear dynamics, symbolic dynamics, and chaos theory, revealing nontrivial correlations, entropy measures, and fractal-like structures in prime distributions. Such approaches aim to address a fundamental question: whether prime numbers are truly random or governed by an underlying deterministic mechanism akin to quantum chaos or quasiperiodic systems.

Recent advances in this direction have been further stimulated by the wide-ranging applications of prime numbers in cryptography, quantum computation, and complex systems theory. Notably, the quantum-mechanical interpretation of prime numbers was initiated by G. Mussardo [9], paving the way for interdisciplinary studies that bridge number theory with quantum mechanics and nonlinear dynamics. These developments underscore the relevance of nonlinear frameworks in uncovering hidden dynamical structures underlying prime number distributions.

Recently, Torquato et al [10] demonstrated that primes exhibit hyper-uniformity, a hidden multiscale order characteristic of quasicrystals and disordered physical systems. From a mathematical-physics perspective, Berry and Keating [2] proposed that prime fluctuations resemble the energy spectra of chaotic quantum systems, with prime spacing statistics following the Gaussian Unitary Ensemble through their connection to the zeros of the Riemann zeta function. Complementary approaches [4, 5] treat prime sequences as symbolic dynamical systems, where entropy measures reveal maximal complexity and fractal analyses of prime gaps uncover $1/f$ noise [6], hallmarks of nonlinear systems with long-range correlations. Together, these results strongly suggest that prime number distribution is governed by an intrinsic nonlinear dynamical structure rather than simple randomness.

Motivated by these observations, we investigate the distribution of prime numbers within a nonlinear dynamical framework. As an extension of our earlier work [11], we construct the lower and upper bounds for the prime counting function and then prime density, which enable a more accurate determination of the interaction potentials experienced by particles represented through a single-particle wave function [12] associated with prime numbers. The resulting interaction potentials corresponding to the two bounds are inherently nonlinear and exhibit contrasting characteristics. We therefore perform a nonlinear dynamical analysis of the system, examining the resulting trajectories, equilibrium points, their stability properties, and the associated bifurcation dynamics within a classical Hamiltonian framework.

The manuscript is organized as follows. In Section-2, we construct of lower and upper bounds for the prime counting function. Section-3 is devoted to the formulation of corresponding bounds for the prime density. In Section-4, we derive the interaction potential associated with prime numbers and analyse the resulting fixed-point structure and phase-space flow. The bifurcation phenomena arising from this framework are examined in Section-5. Finally, the conclusions are presented in Section-6.

2. New bounds on Prime counting function:

Consequent to the declaration of Euclid that there are infinitely many primes i.e., $\pi(x) = \sum_{p \le x} 1$, in the late 18th and early 19th century C. F. Gauss, A.M. Legendre, and P Chebyshev conjectured that the prime counting function can be expressed [13] by the logarithmic integral $\pi(x) \sim li(x) = \int_0^x dt/_{lnt}$ as $x \to \infty$. In 1896, Poussin and Hadamard independently [14, 15] proved the prime number theorem (PNT) and showed that the ratio $\pi(x)/(x/lnx)$ has the limit 1 as $x \to \infty$. It is worth pointing out here that the logarithmic integral can be expressed as $li(x) = \frac{x}{logx} \sum_{k=0}^{\infty} \frac{k!}{(lnx)^k}$. Selecting only the first term in the series, the prime counting function can be approximated as $(x) \approx \frac{x}{lnx}$. To comprehend the accuracy of these functions, the prime counting function represented through $li(x)$ and $\frac{x}{lnx}$ produce an error of 20.50% and -13.14% respectively at x = 100 which decreases to 0.051% and -6.64% respectively for $x = 10^7$. As discussed above, while the prime counting function expressed via the logarithmic integral exhibits larger errors for small values of x, these errors diminish as $x \to \infty$. In contrast, the approximation using $\frac{x}{lnx}$ consistently underestimates $\pi(x)$, with a notably higher relative error even at large values of x. To achieve more accurate approximations of it across the full range of x, considerable efforts [16, 17] have been devoted to establishing reliable upper and lower bounds. In our previous work [11], we proposed such bounds by retaining terms up to the third order in the expansion of $li(x)$, albeit with modified coefficients, yielding improved estimates of the prime counting function,

$$\frac{x}{ln\,x} + \frac{x}{(lnx)^2} + c_1 \frac{x}{(lnx)^3} \le \pi(x) \le \frac{x}{\ln x} + \frac{x}{(lnx)^2} + c_2 \frac{x}{(lnx)^3} \qquad (1)$$

The constants were determined to be $c_1 = -1.881$ and $c_2 = 2.43$ for $x \ge 2$. The resulting lower bound exhibits consistently negative errors, whereas the upper bound shows consistently positive errors across the entire range $x \ge 2$.

Table-1 presents a comparison of these bounds, as obtained from Eq. (1), with the exact values of the prime counting function. It is evident from the table that $\pi_l(x)$ and $\pi_u(x)$ provide significantly tighter lower and upper bounds, respectively, with reduced errors relative to the exact prime counts. Specifically, the errors in $\pi_l(x)$ and $\pi_u(x)$ are -2.5884% and 30.1557% at x = 29 (the 10th prime), which decrease to -0.4119% and 0.0218% at $x = 2.99\times10^{13}$ (the $10^{12\text{th}}$ prime). These results indicate that $\pi_l(x)$ and $\pi_u(x)$ provide more realistic and reliable bounds on the distribution of prime numbers along the number line.

Nth prime	Position	$\pi_l(x)$	Error (%)	$\pi_u(x)$	Error (%)
29	10^1	9.742	-2.5884	13.016	30.1557
541	10^2	95.539	-4.4605	104.8960087	4.8960
7919	10^3	959.818	-4.0182	1007.0077	0.7008
104729	10^4	9716.553	-2.8345	10008.88069	0.0888
1299709	10^5	98006.214	-1.9938	100014.5373	0.0145
15485863	10^6	985475.55	-1.4525	1000188.216	0.0188
179424673	10^7	9888368.886	-1.1163	10001046.68	0.0105
2038074743	10^8	99126881.76	-0.8731	100018976.9	0.0189
22801763489	10^9	992968729.6	-0.7031	1000214351	0.0214
252097800623	10^{10}	9942161276	-0.5784	10002224155	0.0222
2760727302517	10^{11}	99515470855	-0.4845	100021745449.438	0.0218
29996224275833	10^{12}	995880386596.062	-0.4119	1000207631010.15	0.0208

Table-1: Comparison of our estimated lower $\pi_l(x)$ and upper $\pi_u(x)$ bound from Eq. (1) with the exact value of the prime counting function (same as prime position).

3. Density for primes:

To construct a quantum mechanical system representing prime numbers [11], one can derive a probability density corresponding to the primes as a function of x in one dimension, based on the prime counting function. The associated wave function is then obtained from this probability density through standard quantum-mechanical considerations. The average density of primes in the vicinity of a number x, as predicted by the prime number theorem, is given by $\rho(x) = {}^{1}/_{lnx}$,

which exhibits errors comparable to those of the prime counting function itself. To achieve a more accurate representation of the prime density, we define a boundary derived from the lower and upper bounds of the prime counting function as,

$$\rho_l(x) = \frac{1}{lnx}\left(1 + \frac{1}{lnx} - \frac{1.881}{(lnx)^2}\right) \quad (2)$$

$$\rho_u(x) = \frac{1}{lnx}\left(1 + \frac{1}{lnx} + \frac{2.43}{(lnx)^2}\right) \quad (3)$$

To gain a better understanding of the prime density, we compared the results of Eq. (2) and (3) with the actual prime density, as shown in fig. 1. In the figure, the black line represents the actual prime density, while the blue dashed line and green dot-dashed line correspond to $\rho_u(x)$ and $\rho_l(x)$, respectively. The figure clearly demonstrates that $\rho_l(x)$ and $\rho_u(x)$ closely approximate the actual prime density and effectively provide lower and upper bounds across the entire range $x \geq 2$.

From the probability density, the single-particle wave functions $\psi_l(x)$ and $\psi_u(x)$ representing the lower and upper bound is obtained by taking the square root of the corresponding density functions as:

$$\psi_l(x) \propto \sqrt{\rho_l(x)} = A\sqrt{\frac{1}{lnx}\left(1 + \frac{1}{lnx} - \frac{1.881}{(lnx)^2}\right)} \quad (4)$$

And

$$\psi_u(x) \propto \sqrt{\rho_u(x)} = B\sqrt{\frac{1}{lnx}\left(1 + \frac{1}{lnx} + \frac{2.43}{(lnx)^2}\right)} \quad (5)$$

A and *B* are the normalization constants and can be determined within a finite limit of 2 to b ($b < \infty$). However, these constants cancel out in subsequent calculations and therefore do not affect the analysis.

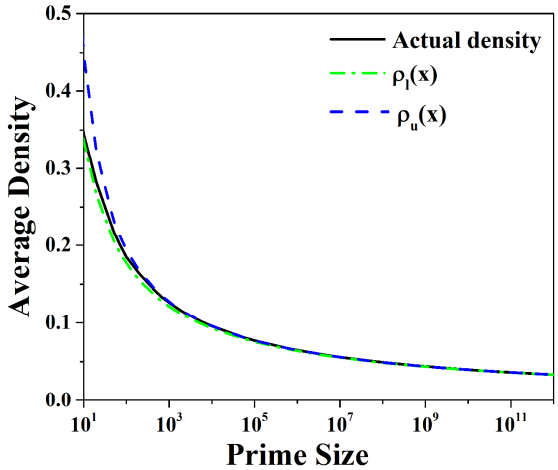

Figure-1: The plot of average density for primes as a function of *x*. The black line indicated actual data of prime density. The blue dashed line and green dot-dashed line represent $\rho_l(x)$ and $\rho_u(x)$ respectively.

4. Interaction potential between primes:

By associating prime number with a single-particle wave function, as described in eq. (4) and (5), the interaction potential experienced by these particles can be derived using the Schrödinger equation [11]. In this framework, a simple quantization scheme is adopted in which prime numbers are treated as the position operators of a quantum system. The resulting potentials corresponding to both the lower and upper bounds are inherently nonlinear and exhibit distinct interaction characteristics. Here, we analyse the nonlinear features of these potentials [13] and examine the corresponding trajectories from a classical perspective [18, 19].

4.1. Derivation of interaction potential from lower bound of wave function:

By using the wave function $\psi_l(x)$ given in eq. (4) in the Schrodinger equation, we determine the potential function $v_l(x)$. Taking $\hbar^2/2m = 1$ and E = 0, we have $v_l(x)$ as

$$v_l(x) = \frac{1}{(2x\,lnx)^2}\left(\frac{1}{lnx}+\frac{1}{(lnx)^2}-\frac{1.881}{(lnx)^3}\right)^{-1}\left[1+\frac{4}{lnx}+\frac{0.357}{(lnx)^2}-\frac{22.572}{(lnx)^3}-\frac{\left(\frac{1}{lnx}+\frac{2}{(lnx)^2}-\frac{5.643}{(lnx)^3}\right)^2}{2\left(\frac{1}{lnx}+\frac{1}{(lnx)^2}-\frac{1.881}{(lnx)^3}\right)}\right] \qquad (6)$$

4.2. Derivation of interaction potential from upper bound of wave function:

The wave function $\psi_u(x)$ given in Eq. (5) is used in the Schrodinger equation to get the potential function $v_u(x)$. By accepting $\hbar^2/2m = 1$ and E = 0, we derive $v_u(x)$ as,

$$v_u(x) = \frac{1}{(2x\,lnx)^2}\left(\frac{1}{lnx}+\frac{1}{(lnx)^2}+\frac{2.43}{(lnx)^3}\right)^{-1}\left[1+\frac{4}{lnx}+\frac{13.29}{(lnx)^2}+\frac{29.16}{(lnx)^3}-\frac{\left(\frac{1}{lnx}+\frac{2}{(lnx)^2}+\frac{7.29}{(lnx)^3}\right)^2}{2\left(\frac{1}{lnx}+\frac{1}{(lnx)^2}+\frac{2.43}{(lnx)^3}\right)}\right] \qquad (7)$$

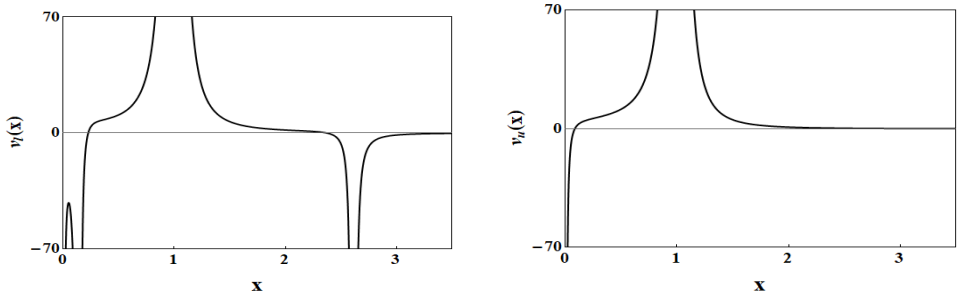

(a) **(b)**

Figure-2: Plot of potentials w.r.t *x*. (a) based on Eq. (6) for lower bound and (b) for upper bound based on Eq. (7).

It is worth noting that the Heisenberg uncertainty principle implies the existence of infinitesimal energy for systems with infinite uncertainty in particle position and time. Equivalently, one can interpret this as infinite freedom in space and time being a characteristic of a zero-energy entity. At $x = 1$, where no prime numbers exist, both the potentials and wave functions diverge. However, within the domain of prime numbers (2 to ∞), the range of the potentials given by Eq. (6) and (7) decreases from 1.838 to 0 and 1.047 to 0, respectively. These potentials are singular (non-regular) [18], as illustrated in Fig. 2. In classical mechanics, a particle subject to such a potential would reach the singularity with infinite velocity. Figure 2(a) shows that the potential derived from the lower bound of the wave function is unstable for $x < 3$ and lies below the number line as $x \to \infty$, indicating that the corresponding force (the negative gradient of the potential) is attractive. In contrast, the upper-bound potential exhibits singularities at x=0, 1 and lies above the number line as it approaches infinity. Figure 2(b) confirms that the associated force in this case is repulsive. This contrasting behaviour of the potentials effectively delineates the lower and upper bounds along the number line and converges at infinity. Given the nonlinear nature of both interaction potentials, one can further explore the hidden nonlinear dynamics [18] underlying the distribution of prime numbers through the corresponding classical Hamiltonian system.

4.3. Phase trajectory and position of zeros on the line:

Considering the nonlinear behaviour of interaction potential $v_l(x)\ and\ v_u(x)$, we study the flow of fixed points or zeros on the real line and its bifurcation

phenomena [18]. To analyse its nonlinearity, we construct the classical Hamiltonian [19] of a single particle system of units as mentioned earlier with $m = 1$, based on the potential functions of the problem in the phase space of x and p. The momentum based on $v_l(x)$ and $v_u(x)$ of the single particle are derived as,

$$\dot{x} = \pm\sqrt{2(E - v_l(x)} \quad (8)$$

$$\dot{x} = \pm\sqrt{2(E - v_u(x)} \quad (9)$$

The trajectories and fixed points play a vital role in nonlinear dynamics. Hence, we plot in fig.3 and fig. 4 the phase trajectory for a given energy parameter E using the Eq. (8) and Eq. (9) respectively. To be specific we choose $E = -100, 0, 1, 100$ and analyse the flow of trajectories with zeros on the phase space. For $-\infty < E < -43$, we found five zeros (x_1, x_2, x_3, x_4, x_5) arise naturally in the graph which are indicated by half-filled circles (x is a zero or a fixed point if $\dot{x} = 0$ at that point). As the value of energy parameter E goes to 0, the two zeroes x_1 and x_2 of the left branch come closer and merge nearly at $x_1 = x_2 \approx 0.1353$ whereas in the right branch one fixed point x_5 moves towards right (a finite value). Thus, at $E = 0$, three zeros exist. For $0 < E < \infty$, two zeros approach each other and merge at $x = 1$ for $E \to \infty$.It is worth pointing here that as the energy parameter (also called bifurcation parameter) varies from $-\infty$ to ∞, the position of fixed point oscillates. The flow pattern of the particle is shown with arrow in the graphs. We know that a particle having positive velocity will go away from its position (zero to infinity) and the particle having negative velocity will come back to its position and stay there which can be seen on the right branch of Fig. 3. On the other hand, in the left branch of each graph, it is opposite in nature i.e., if the particle has positive velocity, then it will move to the fixed point and if it has negative velocity, then it will go away from it. As is done in standard nonlinear dynamics study, stability is shown in darkness and instability in emptiness of the small circles drawn at the fixed points. Since the fixed points have both the stable and unstable nature, it can be named as half-stable fixed point [18]. While analysing Eq. (9) and fig. 4, we notice one fixed point for $E \leq 0$ and two fixed points for $E > 0$. For increasing values of E, both the fixed points approach each other and merge at merge at $x = 1$ for $E \longrightarrow \infty$. After studying the oscillation of fixed points on the x-axis, we can undoubtedly say that it's another case of half-stable fixed point. It is worth pointing here that an inbound trajectory obtained in our case can be related to infinite number of outbound trajectories which may be associated with the infinite primes.

5. Bifurcations of zeros for flow on the line:

Since the fixed points are important in describing the nonlinearity, we study the qualitative changes due to the flow of fixed points within the system which is known as bifurcations. In this dynamical system, first we derive the bifurcation equation from Eq. (8) where we study the bifurcation phenomena. For simplification we choose $lnx = y$ and convert the derived bifurcation equations from Eq. (8) and (9) to y with varying energy parameter (E). For $-\infty < E < -43$ five saddle nodes remain between 0 and 3. As E $\longrightarrow$ 0, two fixed point move towards each other, collide and annihilate at $E \approx -6.8248$. At $E = 0$, another saddle node moves towards infinity and for $E > 0$, both the saddle node approaches each other. So, $E = -6.8248$ and 0 can be considered as bifurcation point where there is a splitting into two branches. This point is made clear in fig.5(a) which is plotted in y- space. For $-\infty < E < 0$, the bifurcation seems to be a fold bifurcation or a turning point bifurcation. When we consider the other side of fig. 5 i.e., $0 < E < \infty$, the blue-sky bifurcation appears. It is worth pointing here that as the energy parameter increases from $-\infty$ to ∞, the bifurcation phenomena change from fold bifurcation to blue sky bifurcation [11,42]. Here, the bifurcation equation on the basis of Eq. (8) can be written as,

$$y^5 + 4.5y^4 + 0.476y^3 - 26.096y^2 - 11.958y + 26.536 - 4Ee^{2y}y^2(y^2 + y - 1.881)^2 = 0 \quad (10)$$

Similarly, the bifurcation equation from Eq. (9) appears as,

$$y^5 + 4.5\,y^4 + 17.72\,y^3 + 42.88\,y^2 + 46.875\,y + 44.287 - 4Ee^{2y}y^2(y^2 + y + 2.43)^2 = 0 \quad (11)$$

When we analyse the Eq. (11), we notice that for $E < 0$, there is only one saddle node remaining between 0 and 0.455. At $E = 0$, another saddle node appears from the blue sky and for E > 0, both the saddle node approaches each other. So, $E = 0$ can be considered as bifurcation point where there is a splitting into two branches. This bifurcation seems to be a case of blue-sky bifurcation [18]. Fig. 5(b) in y-space clearly shows the blue-sky bifurcation [11]. Both the insets in fig.5(a) and (b) show the plot in x-space.

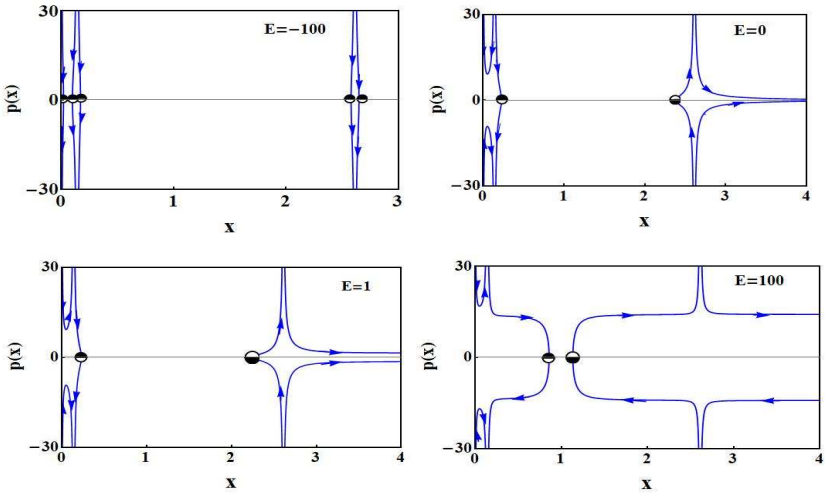

Figure-3: Plot of phase trajectory based on $v_l(x)$. To be specific we choose E as $-100,0,1,100$ and analyse the flow of trajectory on the plane. When $E \to -\infty$, five fixed points are there. When $E \to 0$ two merges to one and only two fixed points left. The two zeroes come closer as $E \to \infty$. The half-filled circle indicates the half stable fixed point.

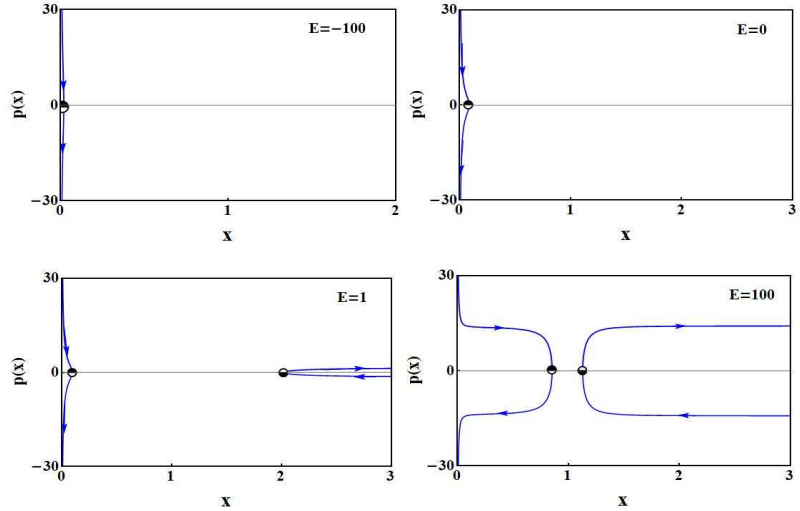

Figure-4: Plot of phase trajectory based on $v_u(x)$for $E = -100,0,1,100$. The half-filled circle indicates the half stable fixed point. As the bifurcation parameter E increases, the fixed points come closer at $x = 1$.

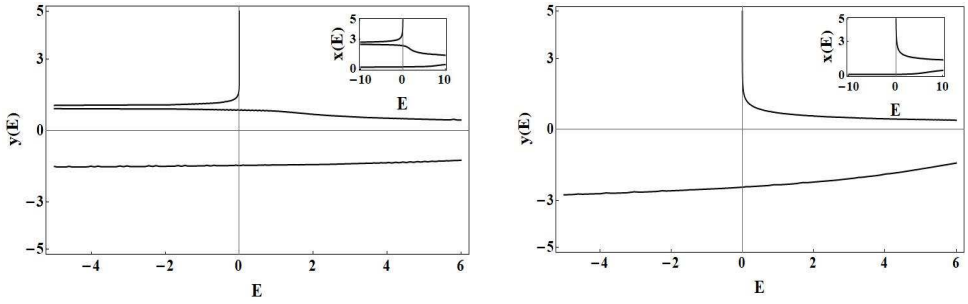

Figure-5: Plot of bifurcation diagrams in y-space. (a) from Eq. (10) shows the combination of fold bifurcation and blue-sky bifurcation whereas (b) from Eq. (11) gives evidence of the blue-sky bifurcation. The insets represent the plot in x-space.

6. CONCLUSION:

Prime numbers exhibit a distinctive pattern along the number line, reflecting a subtle interplay between randomness and regularity. To investigate this behaviour, we employed rigorously constructed lower and upper bounds for both the prime counting function and the associated prime density to characterize the distribution of primes below a given number. The proposed bounds exhibit significantly reduced errors compared to previously reported estimates and are consistently validated by the fact that the exact values of these functions always lie within the derived limits. Furthermore, the nonlinear interaction potentials derived from the bounded prime-density wave functions reveal an intrinsic dynamical structure underlying the distribution of prime numbers. The coexistence of attractive and repulsive regimes, together with the singular and nonlinear nature of these potentials, suggests that prime numbers may be interpreted as emergent features of a complex dynamical system. Within this nonlinear framework, we analysed the trajectories, equilibrium nodes, and their stability properties, as well as the associated bifurcation dynamics arising from the interaction potentials. The study identifies the presence of two distinct types of bifurcations, namely fold bifurcation and blue-sky bifurcation, within the prime number system. Taken together, these results indicate that the distribution of prime numbers is governed by an underlying nonlinear dynamical structure, offering a unified perspective that bridges number theory, quantum mechanics, and nonlinear dynamics. This framework opens new avenues for understanding prime distributions through both classical and quantum mechanical analogies.

Declaration:

The authors have no competing interest to declare that are relevant to the content of this article.

Ethical Approval:

There is no involvement of animals or humans in our study.

Authors' contribution:

Supervision, Methodology, Data preparation and formal analysis, writing-review and editing manuscript [Prasanta Kumar Mahapatra]

Conceptualization, Data preparation, writing- original draft preparation, Graph-plotting [Charli Chinmayee Pal]

Funding:

No funding was received to assist with the preparation of this manuscript.

Data availability statement:

All data generated or analysed during this study are included in this article.

REFERENCES:

[1] A. E Ingham; The Distribution of Prime Numbers, New York: Cambridge University Press (1990).
[2] M. V. Berry and J. P Keating; SIAM Review 41 (2) 236 (1999).
[3] C. M. Bender, C. D. Brody, and M. P. Muller; Phys. Rev. Lett. 118 130201 (2017).
[4] B. Julia; Statistical theory of numbers, in: Luck J.M., Moussa P., Waldschmidt M. (Eds), Number theory and physics, Springer, Berlin, p.276 (1990).
[5] B. Julia; Physica A 203, 425 (1994).
[6] Marek Wolf, Physica A, 274, 1–2, P 149-157, (1999).
[7] S. Okubo; J. Phys. A 31 1049 (1998).
[8] H. C. Rosu; Mod. Phys. Lett. A 18 1205 (2003).
[9] G. Mussardo; arXiv:cond-mat/9712010 (1997).
[10] S Torquato *et al J. Stat. Mech.* 093401 (2018).
[11] C.C. Pal, P.K. Mahapatra & S Mishra; Quantum and classical study of prime numbers, prime gaps and their dynamics. *Quantum Stud.: Math. Found.* (2022).

[12] D. J. Griffiths; Introduction to quantum mechanics, p-19 (Prentice Hall, New Jersey) (1995).

[13] Gauss, C. F.: Werke, *vol. 2 (1st ed.), Göttingen: Teubner, pp. 444-447 (1863).*

[14] J. Hadamard; Bull. Soc. Math. France 14 199-220 (1896).

[15] C. Poussin; Recherchesanalytiques sur la theorie des numbers; Premiere particle; la fonction(s) de Riemann et les numbers (1896).

[16] *L. Schoenfeld; Sharper Bounds for the Chebyshev Functions $\vartheta(x)$ and $\psi(x)$. II, Mathematics of Computation,* ***30*** *(134), 337–360 (1976).*

[17] CAxler C.; New bounds for the prime counting function $\pi(x)$, arXiv: 1409.1780 (2014).

[18] S. H. Strogatz; Nonlinear dynamics and chaos. Perseus books, New York (1994).

[19] H. Goldstein, C. Poole, J. Safko; Classical mechanics, 3rd edn. Addison Wesley, New York (2000).